Unclassified

SECURITY CLASSIFICATION OF THIS PAGE (When Data Entered)

REPORT DOCUMENTATION PAGE

READ INSTRUCTIO BEFORE COMPLETING

1. REPORT NUMBER 4 | 2. GOVT ACC SSION NO. AD-A085 882 | 3. RECIPIENT'S CATALOG NUM

4. TITLE (and Subtitle)
Monitoring Metastable Phases and Grain Structures Derived from Glassy Alloys

5. TYPE OF REPORT & PERIOD
Technical Repor
Oct 78 - Jan

6. PERFORMING ORG. REPORT

7. AUTHOR(s)
Ken-Sue Tan, Thomas Wahl[*] and R. Kaplow

8. CONTRACT OR GRANT NUMBER
N00014-76-C-0[illegible]

9. PERFORMING ORGANIZATION NAME AND ADDRESS
Massachusetts Institute of Technology
Cambridge, Massachusetts 02139

10. PROGRAM ELEMENT, PROJE AREA & WORK UNIT NUMBE

11. CONTROLLING OFFICE NAME AND ADDRESS
Office of Naval Research
Arlington, VA. 22217

12. REPORT DATE
March 24, 198

13. NUMBER OF PAGES
11

14. MONITORING AGENCY NAME & ADDRESS(if different from Controlling Office)

15. SECURITY CLASS. (of this re
Unclassified

15a. DECLASSIFICATION/DOWN SCHEDULE

DTIC ELECTE JUN 2 1980 D C

16. DISTRIBUTION STATEMENT (of this Report)
Unlimited

This document has been approved for public release and sale; its distribution is unlimited.

17. DISTRIBUTION STATEMENT (of the abstract entered in Block 20, if different from Report)

LEVEL

18. SUPPLEMENTARY NOTES
To be published in Proceedings of the 2nd International Conference on Rapid Solidification Processing Principles and Technologies, March 23 1980, Reston, Virginia.

19. KEY WORDS (Continue on reverse side if necessary and identify by block number)
rapid solidification processing
metallic glasses
glass crystallization processing

20. ABSTRACT (Continue on reverse side if necessary and identify by block number)
The glassy phase affords a potentially unique route to achieving new metastable structures with desirable properties. X-ray diffraction, Mö spectroscopy and electron microscopy studies of iron-base alloys show a of potentially useful (and perhaps generally characteristic) behaviors transition from the as-quenched glass towards equilibrium. such as: re glassy states, supersaturated solid solutions, unique metastable compou and phase morphologies, and ultra-fine grain sizes.

DD FORM 1 JAN 73 1473 EDITION OF 1 NOV 65 IS OBSOLETE S/N 0102-LF-014-6601

Unclassified

[*] Smith-Corona Laboratory, Cortland, N.Y.

Monitoring Metastable Phases and Grain Structures Derived from Glassy Alloys

Ken-Sue Tan, Thomas Wahl and Roy Kaplow

Massachusetts Institute of Technology

TECHNICAL REPORT NUMBER 4

March 24, 1980

to

The Office of Naval Research

Contract No. N00014-76-C-0791, NR031-795

To be published in

Proceedings of Conference on
Rapidly Quenched Materials,
Reston, VA. - March 24, 1980

Invited Paper
Proceedings of Conference
on Rapidly Quenched Materials
Reston, VA. - March 24, 1980

Monitoring Metastable Phases and Grain Structures Derived from Glassy Alloys*

Ken-Sue Tan, Thomas Wahl+ and Roy Kaplow

Department of and Center for Materials
Science and Engineering

Massachusetts Institute of Technology

ABSTRACT

The glassy phase affords a potentially unique route to achieving new metastable structures with desirable properties. X-ray diffraction, Mössbauer spectroscopy and electron microscopy studies of iron-base alloys show a number of potentially useful (and perhaps generally characteristic) behaviors in the transition from the as-quenched glass towards equilibrium: (a) precipitation of iron or iron-rich material in crystalline form with high excess interstitial atom content and exceedingly fine grain size, (b) precipitation of metastable compounds, sometimes with the simultaneous appearance of alternate crystalline forms, (c) retention of fine grain size to the temperature of phase equilibrium, (d) phase morphology variability, (e) sensitivity of the kinetics to alloying element and composition control.

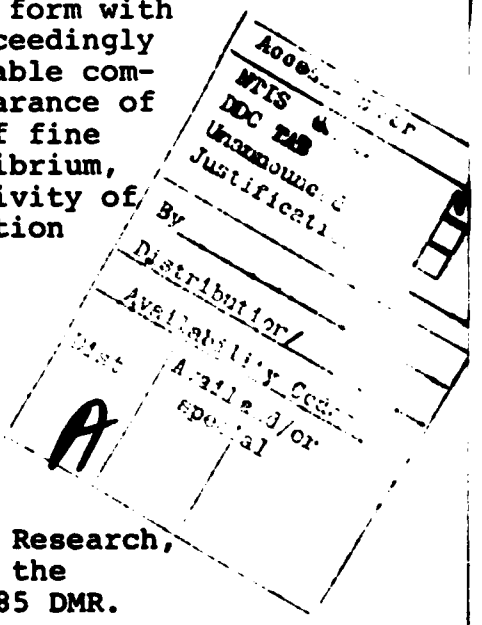

* Research sponsored by the Office of Naval Research, Contract N00014-76-C-0171, NR031-795, and the National Science Foundation, Grant 78-24185 DMR.

+ Present Address: Smith-Corona Laboratory, Cortland, N.Y. 13045.

INTRODUCTION

The iron based glassy alloys, which contain P, B, Si, or C as metalloid elements, have been found to be ferromagnetic (1,2). They are soft magnetic materials (3,4) with excellent magnetic properties (5,6), good mechanical properties (7.8) and high corrosion resistance (9). The glassy states are achieved by extracting the kinetic energy rapidly (10); the cooling is sufficiently quick that the atoms can presumably only make local rearrangements from that which obtains in the liquid, just above the liquidus. If we supply kinetic energy again (by annealing, for example), the atoms will eventually move to lower energy arrangements -- ultimately reaching equilibrium crystalline phases in correspondence with the temperature imposed. The path to equilibrium will in general include a variety of other metastable states, some variations from the as-quenched glass -- but still glass, and other crystalline. In principle, various of these intermediate situations, as regards both the phase structures and the phase morphologies, will not be achievable by other means. Thus, whether or not the "as-quenched" glassy structure is itself preferred for some technical purpose, it also provides a starting point for the application of thermo-mechanical treatments to achieve unique structures which may be desirable. In order to develop that potential, it is necessary to have reliable means for characterizing and interpreting the structural changes occurring; to know -- first of all -- the modes of atomic rearrangements which are likely to occur and to allow monitoring of processing. The purpose of this work has been to examine the structure of the glassy state and, particularly, of its crystallization path towards equilibrium, using the experimental methods of differential scanning calorimetry (DSC), Mössbauer spectroscopy, x-ray diffraction, transmission electron diffraction, and transmission electron microscopy (TEM). In this paper we discuss only Fe-B alloys, of two different compositions.

Materials

The alloys were made and supplied to us by Allied Chemical Company. They were made by Allied's "standard" rapid quenching process of casting onto the outer surface of a rotating drum, in air. The compositions, determined as described later, were $Fe_{83.5}B_{16.5}$ and $Fe_{81}B_{19}$. Both were in the form of long ribbons, with thickness about 40 μm; the former lot is 1 mm wide, the latter is 1 cm wide.

Experimental Samples and Procedures

Samples were cut from the ribbons in lengths appropriate for the various experiments. All annealing was done with the samples in sealed, evacuated and argon-filled pyrex tubes.

For Mössbauer transmission spectroscopy, samples of ∿ 0.75" diameter were assembled on scotch tape with adjacent, parallel ribbon strips. The Mössbauer spectrometer is a standard commercial unit (Austin Scientific); we used it in the constant acceleration, symmetrical velocity mode, with an integral laser interferometer giving velocity calibration points in every sixteenth channel of the 512 channel data logger. X-ray specimens were similarly assembled, but using end-clamps to hold the ribbon pieces, rather than a substrate, to avoid the presence of extraneous material in the beam. Both $Cr_{K\alpha}$ and $Mo_{K\alpha}$ monochromatic x-rays were used for examining the glassy and crystalline phases. The principal diffractometer used allows continuous or step scanning, with both analog (strip chart) and digital (paper tape) data logging.

The DSC runs (Perkin-Elmer model DSC 2) were done with graphite sample chambers. Data was taken at a few different heating rates and also with samples of different weights.

The TEM samples were prepared by electrochemical polishing, using a solution of 10% perchloric acid and 90% methanol. The thinning was done on as-quenched samples; heat treatments for the TEM studies were done in-situ.

Composition Analyses

We found significant discrepancies not only from the nominal compositions (which were presumably just estimates) but also from and among wet chemistry measurements and atomic absorption measurements. The values which we use here were obtained by us using both x-ray diffraction and Mössbauer spectroscopy, in conjunction with the equilibrium phase diagram. Samples were fully crystallized and brought to phase constituency equilibrium by annealing at 727°C for 20 minutes ($Fe_{83.5}B_{16.5}$) or 860°C for a few hours ($Fe_{81}B_{19}$). The equilibrium phases are α-Fe and Fe_2B, which have distinguishable x-ray and Mössbauer signatures. Using all of the x-ray peaks available, that data yields 16.45% B and the best fit to the Mössbauer spectrum yields 16.5% B for lot 1 (nominal 20%). The x-ray data for the wide ribbon yields 19.15% and the Mössbauer, 18.86% (nominal 17%). The most internally consistent atomic absorption results yielded 13.5% and 17.49%, respectively, but only after more divergent results had been questioned.

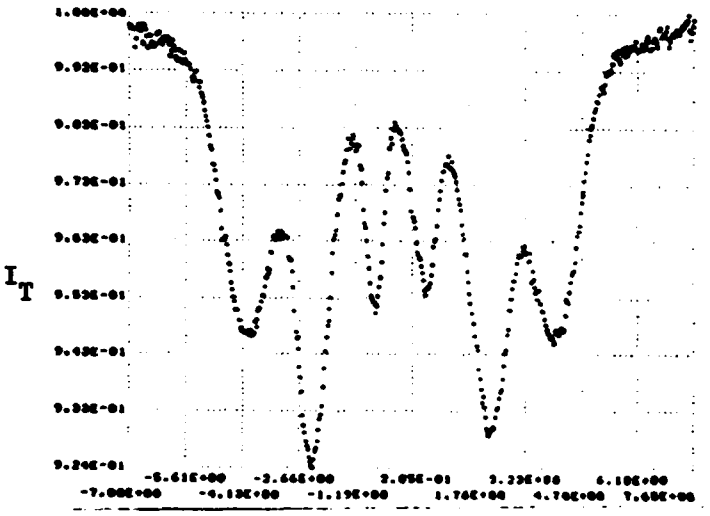

Figure 1. The Mössbauer spectrum of as-quenched $Fe_{83.5}B_{16.5}$.

EXPERIMENTAL RESULTS

The Glass

The Mössbauer spectrum of the 16.5% B as-quenched sample is shown in Figure 1. It shows a broad but well-defined pattern, in which the characteristic "six-line" aspect of ^{57}Fe nuclei in a ferromagnetic material is obvious. The line broadening is certainly caused in part by the distribution of hyperfine fields which results from the distribution of Fe-atom environments associated with the glassy nature of the structure. Interestingly, this spectrum can be fit most simply by just broadening the orthorhombic Fe_3B spectrum measured earlier by Choo and Kaplow (11), while it is not close to the spectra of the equilibrium phases α-Fe or Fe_2B, or any combination of them. Significantly, the broadening required does not wash out an important "signature" of that Fe_3B spectrum, which is due to the existence of two particular and distinct iron atom sites in the structure, with different isomer, electric quadrupole, and magnetic hyperfine interactions. The

visible aspects of these details can be seen in the asymmetry of the glassy spectrum, in terms of peak positions, heights and widths.

A sample annealed at low temperature (250°C for 9 days) shows a Mössbauer spectrum in which the peaks are slightly sharper, which may be attributed to a structural relaxation.

The x-ray diffraction data for the same as-quenched glass yields a pair distribution function generally consistent with that measured earlier (12); without being certain of compositional or primary processing differences it is not useful to postulate about the reality or the meaning of quantitative differences among different experiments. We cannot resolve Fe-B pairs in the largely Fe-Fe dominated main neighbor peak. Making a rough allowance for the contribution of Fe-B neighbors (which is small because of the low scattering factor of boron) we estimate that there are 11.6 Fe-Fe "nearest" neighbors in that peak (centered at 2.52 Å and with a FWHM of 0.46 Å). After annealing for 2 hours at 300°C, there is no visible evidence of crystallization in the x-ray pattern, but some evidence for relaxation in the glass, e.g., sharpening of the near neighbor peak in the RDF (by aobut 3%), consistent with comparable Mössbauer indications.

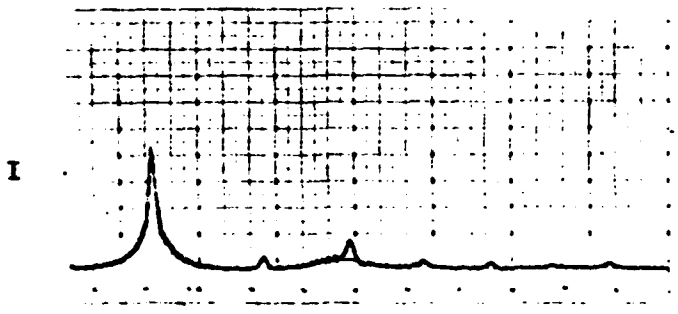

Figure 2. The x-ray diffraction pattern of an $Fe_{83.5}B_{16.5}$ sample, after annealing for 15 hours at 300°C. The crystalline peaks are α-Fe(B) and the diffuse continuum is due to the remaining glass.

Crystallization Sequencing

On further annealing (e.g., at 300°C for longer times or at higher temperatures for correspondingly shorter times) both x-ray and Mössbauer results indicate that α-Fe crystallizes first (in this sample), while the remaining glassy material subsequently transforms to crystalline Fe_3B. Figure 2 shows an x-ray diffraction pattern for the 16.5% B material after annealing at 300°C for 15 hours; the pattern shows a mixture of glass and crystalline α-Fe. At higher temperatures, the metastable Fe_3B boride decomposes to additional α-Fe and Fe_2B. The crystallization behavior as judged by x-ray and Mössbauer measurements is summarized in Table I for the $Fe_{83.5}B_{16.5}$ sample and Table II for the $Fe_{81}B_{19}$ sample. The lattice parameter of α-Fe has also been monitored in the $Fe_{83.5}B_{16.5}$ sample and found to change as a function of heat treatment; this is also shown in Table I, and discussed later. It should be noted that each entry in both of these tables corresponds to a separate sample-treatment; sequential treatments were not used for these data.

Regarding the difference in behavior between the two samples, we point out that in the higher composition alloy (a) there is somewhat more resistance to initial crystallization, (b) when crystallization occurs, the Fe_3B and α-Fe appear more or less at the same time (but with some evidence to indicate

Phases Present in Annealed $Fe_{83.5}B_{16.5}$

Temperature	Time	Phases Present	α-Fe Lattice Constant	Particle Size (Å)
727°C	20 min.	α-Fe + Fe_2B	2.867	1520
	10 min.	α-Fe + Fe_2B	2.868	1254
555°C	2 hrs.	α-Fe + (Fe_3B) + Fe_2B	---	946
525°C	2 hrs.	α-Fe + Fe_3B + Fe_2B	---	712
505°C	2 hrs.	α-Fe + Fe_3B + (Fe_2B)	---	710
480°C	2 hrs.	α-Fe + Fe_3B	---	731
375°C	16 hrs.	α-Fe + Fe_3B	2.8640	581
375°C	8 hrs.	α-Fe + Fe_3B	2.8634	538
375°C	4 hrs.	α-Fe + Fe_3B + (glass)	2.8628	468
375°C	2 hrs.	α-Fe + glass	2.8617	445
375°C	1 hr.	α-Fe + glass	2.8616	484
375°C	0.5 hr.	α-Fe + glass	2.8615	484
350°C	8 hrs.	α-Fe + glass + Fe_3B	2.8617	448
350°C	4 hrs.	α-Fe + glass	2.8616	467
350°C	2 hrs.	α-Fe + glass	2.8608	448
350°C	1 hr.	α-Fe + glass	2.8613	479
350°C	0.5 hr.	α-Fe + glass	2.8614	452
300°C	100 hrs.	α-Fe + glass	2.8610	461
300°C	50 hrs.	α-Fe + glass	2.8610	447
300°C	30 hrs.	α-Fe + glass	2.8610	424
300°C	15 hrs.	α-Fe + glass	2.8608	454

Table II

Phases Present in Annealed $Fe_{81}B_{19}$

Temperature	Time	Phases Present
860°C	3 hrs.	α-Fe + Fe_2B
855°C	1 hr.	α-Fe + Fe_2B + Fe_3B
455°C	4 hrs.	α-Fe + Fe_3B + (Fe_2B)
	3 hrs.	α-Fe + Fe_3B
	2 hrs.	α-Fe + Fe_3B
350°C	10 hrs.	α-Fe + Fe_3B
350°C	4 hrs.	α-Fe + Fe_3B
350°C	3 hrs.	α-Fe + Fe_3B (slight)
350°C	2 hrs.	α-Fe + glass
300°C	15 hrs.	glass + ?

the α-Fe(B) does appear before the Fe_3B and (c) equilibrium is achieved only at higher time/temperature values.

Crystallization Morphology

Particle sizes for the crystallized α-Fe are also shown in Table. 1. These were measured from the broadening of the α-Fe (211) x-ray peaks, using a pure, polycrystalline α-Fe sample as a standard. As seen, the grain size starts at about 450 Å (when we can first clearly see the phase in either the x-ray or Mössbauer patterns). After annealing sufficiently to achieve the equilibrium phase constituents, the average α-Fe grain size is still as small as 1500 Å, showing (as anticipated) that transformation of the glassy phase provides a route to fine grain size material.

TEM studies, on $Fe_{81}B_{19}$ samples, annealed *in situ* at a temperature of 350°C, also show very small α-Fe particles, about a few hundred angstroms in diameter, consistent with the x-ray data. The TEM work also shows much larger isolated Fe_3B particles, inside an α-Fe matrix, as shown in Figure 3, for a sample annealed at 350°C for 3.5 hours. Each such particle appears to be comprised of a number of grains, with a total particle size roughly ten times larger than the α-Fe grains at the same point in time.

Figure 3. A TEM micrograph of an $Fe_{81}B_{19}$ sample, annealed at 350°C for 3.5 hours. A "large" Fe_3B particle, apparently comprised of a number of separate grains, is visible in a matrix of crystalline iron.

Structure of Fe_3B

Fe_3B is a metastable boride, first noted in rapidly quenched (splat-cooled) low boron content iron alloys, where it was said to be orthorhombic, isostructural with Fe_3C, and with lattice parameters a = 5.433 Å, b = 4.454 Å, c = 6.656 Å (13,14). Subsequent work on the metastable boride formed by splat cooling included Mössbauer spectroscopy. The results there showed a well-defined and unique Mössbauer spectrum for that boride, consistent with the numbers and relative occupation of iron atom sites in the orthorhombic structure (11).

In the existing work on the thermal decomposition of Fe-B glasses, there seems now to be a concensus that Fe_3B is the metastable boride product of the decomposition, largely on the basis of x-ray diffraction identification (although Fe_4B has also been suggested) (15). Some have declared the Fe_3B to be the aforementioned orthorhombic form (6,16-19); others declare it is to be tetragonal (a = 8.63 A, c = 4.28 Å) and isostructural with Fe_3P (20-23). Unfortunately, the x-ray powder patterns predicted for these two structures are so similar (especially in a pattern dominated by that of α-iron) that we find it virtually impossible to reliably discriminate between the two in that manner.

On the other hand, the Mössbauer spectra evidence a large difference between these two structures (21,24). The Fe_3B, formed in a $Fe_{81}B_{19}$ sample, annealed, for example, at 350°C for 10 hours, yields a complex spectrum which can be best fit by a combination of 70% of the tetragonal spectrum and 30% of the orthorhombic one, as shown in Figure 4. This is consistent with Franke's (24) and Herold's (25) conclusion, i.e., that both structures exist during the transformation.

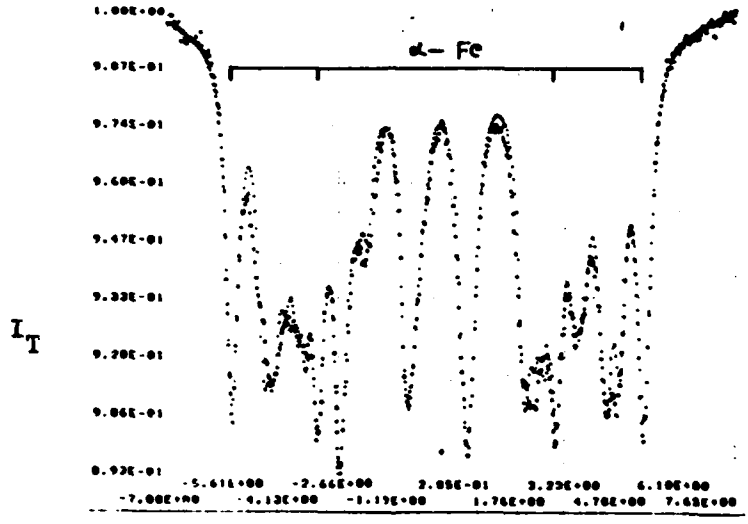

Figure 4. The Mössbauer spectrum of an $Fe_{81}B_{19}$ sample, annealed at 350°C for 10 hours. The "+" points are experimental data and the "." points are a fit using a combination of the spectra of α-Fe, tetragonal Fe_3B and orthorhombic Fe_3B.

By selected area diffraction in the 19.1% B sample we do find diffraction spot patterns corresponding to the orthorhombic phase, e.g., (013) $(41\bar{2})$, but a majority appear to correspond to the tetragonal phase, e.g., $(0\bar{2}1)$, $(\bar{1}11)$, (011), $(1\bar{1}\bar{1})$ $(01\bar{1})$. Figure 5 shows the electron diffraction pattern when the area includes an Fe_3B "cluster", as seen in Figure 3, with patterns corresponding to both structures; when such borides are not visible in the microscopy, only polycrystalline α-Fe diffraction rings appear.

Supersaturation of α-Fe

It was noted in Table I that the lattice parameter of the α-Fe changes with annealing conditions, being smaller the lower the temperature/time condition, but ultimately approaching the exact value for pure iron. These values were measured from the α-Fe (211) reflection, using $Cr_{K\alpha}$ radiation and

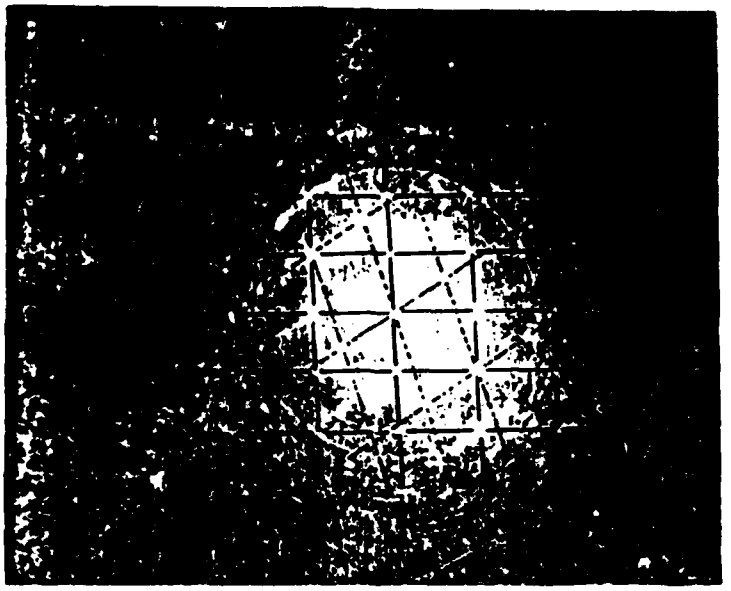

Figure 5. A transmission electron diffraction pattern of the sample shown in Figure 3, from an area including a similar particle. Diffraction patterns are attributable to tetragonal Fe_3B $(00\bar{1})$ [dashed lines] and orthorhombic Fe_3B (013) [solid lines].

a pure iron standard. If boron atoms are trapped in the crystallized iron, the lattice parameter will be bigger if the borons are in interstitial sites and smaller if a sufficient fraction of them are substitutional. The lattice parameter of the equilibrium Fe-B solid solution is said to decrease by about 0.001 Å per percent boron (26). In alloys formed by rapid quenching directly from the melt, with up to 12% B, Ray and Hasegawa (27) report that only crystalline supersaturated α-Fe(B) is obtained with a substitutional ratio of 3 B for 2 Fe. The lattice parameters determined there are a reasonably close extrapolation of the low boron equilibrium values. If the 3 for 2 ratio holds here, then the boron content corresponding to the lowest time/temperature entry in Table I would be ∿ 8%*. In situ electron diffraction results, however, have indicated that the relative lattice parameter of first detected crystalline α-Fe is significantly smaller than the average seen by the x-ray beam. Thus it seems possible that the α-Fe initially crystallizes with all of the local boron trapped in place. Just how near that is to the overall composition depends on the homogeneity in the glass, and in turn on that in the original liquid.

Kinetics

In Figure 6 and 7 we show the DSC data for $Fe_{83.5}B_{16.5}$ and $Fe_{81}B_{19}$, respectively, for the temperature range 650 - 800°K with a heating rate of 20°/min. Data at 5°/min. and 10°/min. differ only in relatively small

* These particular data were on samples aged at room temperature for about six months. Less accurate data taken immediately after the treatment indicated a smaller lattice constant and hence a larger boron content.

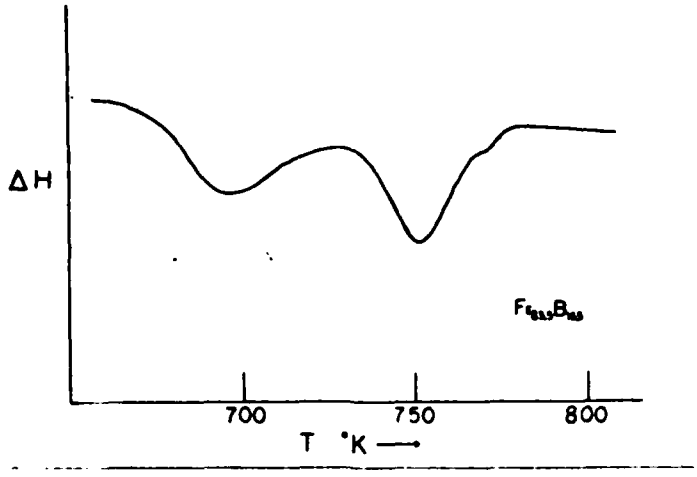

Figure 6. The DSC data for an $Fe_{83.5}B_{16.5}$ sample over the range 650°K to 800°K (20°/min. heating rate).

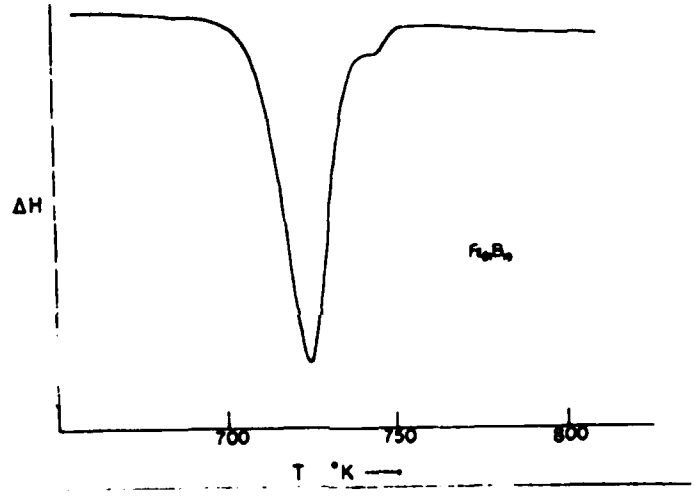

Figure 7. The DSC data for an $Fe_{81}B_{19}$ sample over the range 650°K to 800°K (20°/min. heating rate).

quantitative respects. First, we note the change from the two peak aspect of the first sample to the one peak aspect in the second. This is in strong qualitative agreement with the results of Walter, Bartram and Mella (28). We have seen no evidence ourselves for the "two amorphous phase" model which they propose, but these results are fully consistent with the different behavior of the two alloys with respect to crystallization phase sequencing. Thus, comparing the DSC curves to Table I, we attribute the first "peak" in Figure 6 to the crystallization of α-Fe and the second to Fe_3B. In the higher composition alloy (Table II and Figure 7) the two phases appear more nearly simultaneously. We do not see any clear sign of Fe_2B formation in DSC curves up to 950°K. (Nor do we expect to, because of the relatively large temperature range of that transformation that is indicated by the isothermal data.) The extra small shoulder on the high temperature side in both patterns seems large enough to be real, but we are not certain of its source.

The atomic fraction of α-Fe is proportional to the intensity of its characteristic peaks in Mössbauer spectrum. From this, the volume fraction x(t) formed at the time t can be calculated. Log (-log(1-x)) vs. log t for

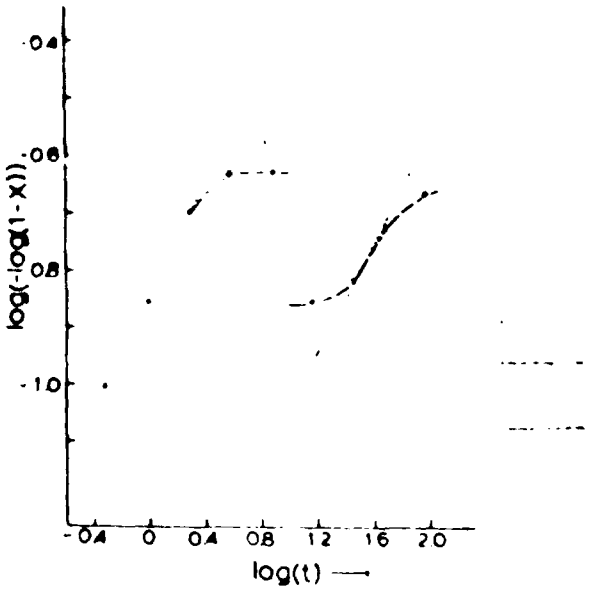

Figure 8. Crystallization kinetics of α-Fe in an originally glassy $Fe_{83.5}B_{16.5}$ sample. Curve on left at 350°C to 8 hours; curve on right at 300°C to 100 hours.

two series of heat treatments of the $Fe_{18.5}B_{16.5}$ samples has been plotted in Figure 8, where x is the volume fraction of the α-Fe phase. At 350°C, the transformation initially follows the Avrami equation but then saturates at x = 0.42. This value is consistent with a pseudo-equilibrium between the α-Fe(B) phase and an Fe_3B phase, deficient in boron to compensate for the boron atoms still in the α-Fe(B). At T = 300°C, we get an unexpectedly large fraction of α-Fe at short times; this may be attributable to inhomogeneous nucleation, as postulated by Koster (29). Nonetheless, the transformation again tends to saturate at x = 0.42.

CONCLUSIONS

The crystallization process in Fe-B glasses is clearly sensitive to boron content. Crystallized iron forms initially highly supersaturated with boron, but later achieves a pseudo-equilibrium with metastable Fe_3B. The latter phase exists simultaneously in both the orthorhombic and tetragonal forms, isostructural with Fe_3C and Fe_3P, respectively. Small α-Fe grain sizes are maintained throughout the crystallization process, ranging from about 300 Å to perhaps 1500 Å when α-Fe + Fe_2B equilibrium is achieved.

ACKNOWLEDGEMENTS

This work was sponsored by the Office of Naval Research, under Contract N00014-76-C-0171, NR031-795, and in part by the National Science Foundation, under Grant 78-24185 DMR.

REFERENCES

1. C. D. Graham, Jr., S. T. Egami, Ann. Rev. Mater. Sci., Vol. 8, p. 423 (1978).

2. C. L. Chien, R. Hasegawa, Phys. Rev. B., Vol. 16, No. 5, p. 2115 (1977).

3. [illegible]
J. of Appl. Phys., Vol. 47, No. 10, p. 4660 (1976).

4. R. C. O'Handley, R. Hagegawa, R. Ray and C. P. Chou, Appl. Phys. Letters, Vol. 29, No. 6, p. 15 (1976).

5. T. Egami and S. D. Dahlgren, J. Appl. Phys. 49(3) (1978).

6. R. Hasegawa, R. C. O'Handley, L. E. Tanner, R. Ray and S. Kavesh, Appl. Phys. Letters, Vol. 29, No. 3 (1976).

7. L. A. Davis, R. Ray, C. P. Chou and R. C. O'Handley, Scripta Met., Vol. 10, p. 541 (1976).

8. L. Davis, Metallic Glasses, Metals Park, Ohio, Am. Soc. Met., p. 190 (1977).

9. T. Masumoto and K. Hashimoto, Ann. Rev. Mater. Sci., 8, p. 215 (1978).

10. P. Duwez, Ann. Rev. Mater. Sci., Vol. 6 (1976).

11. W. K. Choo and R. Kaplow, Metallurgy Trans. A, Vol. 8A, p. 417 (1977).

12. Y. Wasaeda and H. S. Chen, Phys. Stat. Sol. (A), Vol. 49, p. 387 (1978).

13. R. Ruhl, M.I.T., Sc.D. Thesis, Dept. of Metallurgy, 1967.

14. R. P. Elliott, Constitution of Binary Alloys, First Supplement, New York, McGraw-Hill, 1965.

15. U. Köster and U. Herold, Scripta Metallurgica, Vol. 12, p. 75 (1978).

16. M. Takahashi and M. Koshimura, Japan J. Appl. Phys., Vol. 16, No. 9 (1977).

17. C. [illegible]. Chien, Phys. Rev. B., Vol. 18, No. 3, p. 1603 (1978).

18. H. Franke and M. Rosenberg, IEEE Trans. on Mag., Vol. Mag-14, No. 5 (1978).

19. B. G. Lewis, H. A. Davis and K. D. Ward, Rapidly Quenched Metals III, Vol. 1, p. 325 (1978).

20. H. Franke, U. Herold, U. Köster and M. Rosenberg, J. MMM, 9, p. 214 (1978).

21. J. L. Walter, S. F. Bartram and R. R. Russell, Metallurgical Trans. A, Vol. 9A, p. 803 (1978).

22. J. L. Walter and S. F. Bartram, ref. 19, p. 307.

23. T. Kemey, I. Vincze, B. Fogarassy and S. Arajs, Ref. 19, p. 221.

24. H. Franke, U. Herold, U. Köster and M. Rosenberg, Ref. 19, p. 159.

25. U. Herold and U. Köster, Z. Metallkde, Vol. 69, p. 326 (1978).

26. A. K. Shevelev, Soviet Phys. "Doklady", Vol. 3, p. 1254 (1958).

27. R. Ray and R. Hasegawa, Soilid State Comm., Vol. 27, p. 371 (1978).

28. J. L. Walter, S. F. Bartram and I. Mella, Mat. Sci. and Eng., Vol. 36, p. 193 (1978).

29. U. Köster, communication at "Annual Meeting of Materials Research Soc.", Nov. 1979.